Immersion Calorimetry as a Tool To Evaluate the Catalytic Performance of Titanosilicate Materials in the Epoxidation of Cyclohexene

ARTICLE *in* LANGMUIR · FEBRUARY 2011

Impact Factor: 4.46 · DOI: 10.1021/la104808v · Source: PubMed

Langmuir

ARTICLE

pubs.acs.org/Langmuir

Immersion Calorimetry as a Tool To Evaluate the Catalytic Performance of Titanosilicate Materials in the Epoxidation of Cyclohexene

Jarian Vernimmen,*[,†] Matteo Guidotti,[‡] Joaquin Silvestre-Albero,[§] Erika O. Jardim,[§] Myrjam Mertens,[∥] Oleg I. Lebedev,[⊥,#] Gustaaf Van Tendeloo,[#] Rinaldo Psaro,[‡] Francisco Rodríguez-Reinoso,[§] Vera Meynen,[†] and Pegie Cool[†]

[†]Laboratory of Adsorption and Catalysis, Department of Chemistry, University of Antwerp, CDE, Universiteitsplein 1, B-2610 Wilrijk, Belgium

[‡]CNR-Istituto di Scienze e Tecnologie Molecolari, via G. Venezian 21, 20133 Milano, Italy

[§]Laboratorio de Materiales Avanzados, Departamento de Química Inorgánica-Instituto Universitario de Materiales, Universidad de Alicante, Ctra. San Vicente s/n, E-03690 Alicante, Spain

[∥]Flemish Institute for Technological Research (VITO N.V.), Boeretang 200, B-2400 Mol, Belgium

[⊥]CRISMAT, UMR 6508, CNRS-ENSICAEN, 6 Bd Marechal Juin, 14050 Caen, France

[#]EMAT, Department of Physics, University of Antwerp, CGB, Groenenborgerlaan 171, B-2020 Antwerpen, Belgium

ABSTRACT: Different types of titanosilicates are synthesized, structurally characterized, and subsequently catalytically tested in the liquid-phase epoxidation of cyclohexene. The performance of three types of combined zeolitic/mesoporous materials is compared with that of widely studied Ti-grafted-MCM-41 molecular sieve and the TS-1 microporous titanosilicate. The catalytic test results are correlated with the structural characteristics of the different catalysts. Moreover, for the first time, immersion calorimetry with the same substrate molecule as in the catalytic test reaction is applied as an extra means to interpret the catalytic results. A good correlation between catalytic performance and immersion calorimetry results is found. This work points out that the combination of catalytic testing and immersion calorimetry can lead to important insights into the influence of the materials structural characteristics on catalysis. Moreover, the potential of using immersion calorimetry as a screening tool for catalysts in epoxidation reactions is shown.

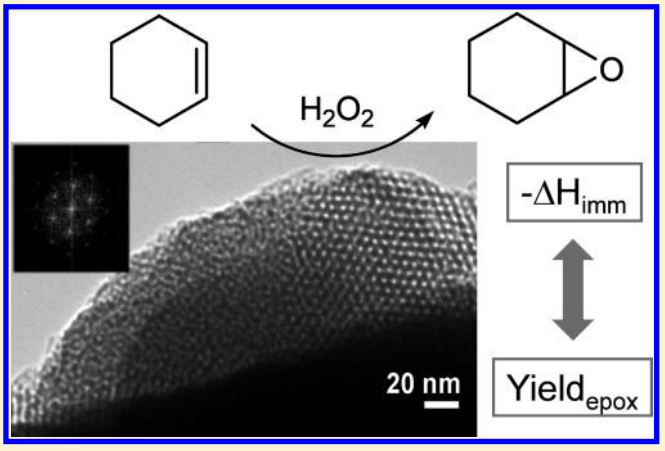

1. INTRODUCTION

The microporous titanosilicate, titanium-silicalite-1 (TS-1, MFI structure),[1] is considered as one of the most versatile redox catalysts available. TS-1 currently finds application in a wide series of oxidation processes with H_2O_2 at both benchmark and industrial scale,[2,3] such as the epoxidation of alkenes,[4] hydroxylation of aromatics,[5−7] cyclization reactions,[8] oxidation of alcohols[9,10] and ammoximation of ketones.[11] The remarkable efficiency of TS-1 is attributed to (i) the isolation of Ti sites, preventing the undesired decomposition of H_2O_2, and (ii) the hydrophobic character of the lattice, enabling the preferential adsorption of the hydrophobic substrates also in the presence of water.[12] However, a major drawback of TS-1 is that its microporous nature causes diffusion limitations or restricted accessibility for viscous fluids and bulky molecules.[13] Mesoporous materials, like Ti-MCM-41 and Ti-SBA-15, on the other hand, offer an enhanced diffusion and improved accessibility for large molecules and viscous fluids[13] but are in many ways (e.g., stability, catalytic activity, selectivity) inferior to zeolites.[14,15] Therefore, the combination of zeolites and mesoporous networks has attracted a lot of attention during the past decade. Examples of such materials are Ti-MMM-1,[16] MTS-9,[17] MTS-5, and MTS-8.[18] In order to evaluate the catalytic potential of combined zeolitic/mesoporous materials and to compare their performance with conventional titanosilicates (for example, TS-1 and Ti-MCM-41), it is very important that the structural characterization of all materials is executed thoroughly. From a catalytic point of view, the dispersion of the active sites, the

Received: December 3, 2010
Revised: January 24, 2011
Published: February 23, 2011

accessibility of these sites, the surface area available to the reactants, and the pore structure are of primordial importance. An equally important aspect is the surface chemistry of a catalyst, more specifically the interactions of the reactants with the active sites of the catalyst. Of course, it is clear that the surface chemistry is strongly related with the structural characteristics of the catalyst. Thus, a thorough structural and surface characterization is necessary in order to correlate the catalytic activities of the materials directly with their structural differences.

An excellent technique for the investigation of the interaction of molecules with a solid surface is immersion calorimetry.[19,20] Here, the heat of immersion of a solid immersed into a nonreacting liquid is determined. The heat of immersion depends on the surface area available to the liquid, the porosity of the solid, and the specific interaction of the liquid molecules with the solid surface. In practice, this means that by using a wide variety of liquids, immersion calorimetry can be applied for the assessment of the pore size distribution, acidity, basicity, and surface polarity of a solid material.[19,21−25] However, reports in which catalytic testing is combined with immersion calorimetry are very scarce.[26] Moreover, to the best of our knowledge, there is no literature available that explicitly combines the catalytic conversion of a specific molecule with immersion calorimetry of the same molecule.

In this work, we report for the first time the combined use of immersion calorimetry and a catalytic test reaction for the comparative evaluation of different Ti-containing siliceous catalysts. The catalytic results for the epoxidation of cyclohexene are correlated with the heat of immersion of cyclohexene for the different catalysts, namely, TS-1, Ti-containing MCM-41 (obtained by grafting a Ti(IV) inorganic precursor), and three types of combined zeolitic/mesoporous materials. The goal is to demonstrate that immersion calorimetry can be a very useful extra tool for the interpretation of catalytic test results. Moreover, the combination of catalytic testing and immersion calorimetry can lead to important insights into the interplay of the structural and surface characteristics of titanosilicates on the epoxidation reaction.

2. EXPERIMENTAL SECTION

2.1. Synthesis of the Catalysts. TS-1 (titanium-silicalite-1) was prepared by adjusting the TS-1 precursor procedure by Meng et al.[17]

The TS-1 precursor solution was prepared by mixing 7.5 mL of TPAOH (tetrapropylammonium hydroxide, 1.0 M aqueous solution, Aldrich) with 10.5 mL of distilled water. Then, 300 μL of TBOT (titanium butoxide, 99%, Acros) and 5.6 mL of TEOS (tetraethyl orthosilicate, 98%, Acros) were added. The initial molar ratio is 1 TBOT/30 TEOS/8 TPAOH/1050 H_2O. The mixture was stirred for 1.5 h at room temperature. In order to obtain the full grown TS-1 microporous titanosilicate, this precursor solution was subjected to a hydrothermal treatment for 7 days at 150 °C in a Teflon-lined autoclave. After centrifugation, washing, and drying of the final product, a calcination procedure was carried out. The materials were calcined under ambient atmosphere at 550 °C for 6 h with a heating rate of 1 °C/min.

Meso-TSM, a newly developed combined zeolitic/mesoporous titanium-incorporated siliceous material, was prepared by applying a one-pot templating strategy, based on an adjusted TS-1 synthesis. Here, part of microtemplate (TPAOH) was replaced by a mesopore templating agent (cetyltrimethylammonium bromide, CTMABr), resulting in a mixture with an initial molar ratio of 1 TBOT/30 TEOS/4 TPAOH/4 CTMABr/1050 H_2O. Therefore, the acronym "meso-TSM" is derived from *meso*porous material with *TS*-1 characteristics, synthesized by using the mesotemplate CT*M*ABr. A typical synthesis procedure proceeds as follows: 1.4 g of CTMABr (Acros) was dissolved in 13.5 mL of distilled water. Then, 3.75 mL of TPAOH was added to the surfactant solution during stirring. After that, 300 μL of TBOT and 5.6 mL of TEOS were added under vigorous stirring. The stirring period of 1.5 h at room temperature was followed by a hydrothermal treatment of 2 days at 150 °C in a Teflon-lined autoclave. After filtrating, washing, and drying of the final product, a calcination procedure (as described above) was carried out.

SBA-TS-15, a Ti-incorporated siliceous material, was synthesized via the postsynthetic deposition of TS-1 nanoparticles. The SBA-15 support was synthesized by a procedure, described by Meynen et al.,[27] and subsequently calcined. The TS-1 nanoparticles (TS-1 clear precursor solution) were prepared by following the first step of the TS-1 synthesis (described above). After the stirring period of 1.5 h at room temperature, the mixture was subjected to a hydrothermal aging period of 3 days at 70 °C (instead of 7 days at 150 °C). This was done in a round-bottom flask which was equipped with a condenser and placed in an oil bath. SBA-TS-15 was obtained by performing an incipient wetness impregnation; i.e., a certain volume of TS-1 precursor solution was added to dry, calcined SBA-15. Two types of SBA-TS-15 materials were prepared: SBA-TS-15-pH 13 and SBA-TS-15-pH 1. The former structure was obtained by adding 7.5 mL of the basic TS-1 precursor solution (pH = 13) to 0.6 g of dry SBA-15. For the SBA-TS-15-pH 1 material, 7.5 mL of an acidified TS-1 solution (pH = 1) was added to 0.6 g of dry SBA-15. The acidification was performed by adding 0.5 mL of concentrated HCl (37%, Acros) to 10.0 mL of TS-1 precursor solution. After impregnation, the SBA-TS-15 materials were dried and calcined under identical conditions as described above.

Ti-MCM-41 was prepared by grafting titanocene dichloride onto the surface of calcined MCM-41,[28] according to a methodology previously reported.[29] $Ti(Cp)_2Cl_2$ was dissolved in chloroform and allowed to diffuse into silica. The solid was then exposed *in situ* to triethylamine to activate the nucleophilic substitution of surface silanols with titanocene. After filtration, Ti(IV) active centers were obtained after calcination under dry oxygen at 550 °C for 3 h.

2.2. Characterization. The N_2-sorption measurements at −196 °C were determined using a Quantachrome Quadrasorb SI automated gas sorption system. Prior to measurements, the samples were outgassed under vacuum during 16 h at a temperature of 200 °C. The Barret−Joyner−Halenda (BJH) method applied to the adsorption branch of the isotherm was used to determine the pore size distribution. The micropore volume was obtained via the *t*-plot method, while the Brunauer−Emmet−Teller (BET) method was applied to calculate the specific surface area. The total pore volume was determined at P/P_0 0.95.

X-ray diffraction (XRD) measurements were carried out on a PANalytical X'PERT PRO MPD diffractometer with Cu radiation. Also, a bracket stage, a monochromator, and soller slits were used. The measurements were performed in the 2θ mode using a monocrystal with a scanning speed of 0.04°/4 s and measuring in continuous mode.

Electron probe microanalysis (EPMA) was utilized for the determination of the titanium concentration in the samples. The EPMA analyses were preformed on a JEOL JXA 733 apparatus. The coordination of titanium was determined by a UV−vis spectrophotometer (Thermo Electron Evolution 500), equipped with an integrating sphere (RSA-UC-40 diffuse reflectance cell). An average of three scanning cycles was taken with a scanning speed of 120 nm/min and a bandwidth of 2 nm.

Meso-TSM was further characterized by transmission electron microscopy (TEM) and EDX analysis using a Philips CM20 microscope equipped with an Inca X-ray microanalysis unit, operating at 200 kV and having point resolution of 0.27 nm. The TEM sample was prepared by crushing the material in methanol in an agate mortar and dropping this dispersion of finely ground material onto a holey carbon film supported

Table 1. Structural Characteristics of the Different Catalysts[a]

	N_2 sorption					XRD	EPMA
	BET ($m^2\ g^{-1}$)	V_μ ($cm^3\ g^{-1}$)	V_{tot} ($cm^3\ g^{-1}$)	R_{ads} (nm)	isotherm type	MFI zeolite profile	% Ti
TS-1	360	0.11	0.33	–	I	yes	4.1
MCM-41 support	1450	0.00	0.80	1.0	IV	–	–
Ti-MCM-41	1330	0.00	0.99	1.1	IV	–	1.4
SBA-15 support	827	0.15	0.99	3.6	IV	–	–
SBA-TS-15-pH 1	406	0.05	0.42	3.2	IV	no	0.9
SBA-TS-15-pH 13	457	0.08	0.48	3.4	IV	no	1.3
meso-TSM	786	0.00	0.79	1.5	IV	yes	1.2

[a] BET = specific surface area, V_μ = micropore volume, V_{tot} = total pore volume at $P/P_0 = 0.95$, R_{ads} = average pore radius, based on the adsorption pore size distribution, and EPMA = electron probe microanalysis (wt % Ti).

on a Cu grid. Low electron beam intensities and low magnification were applied in order to minimize the electron beam damage of the material. Fourier transformation (FT) of high-resolution TEM (HRTEM) images was performed using Digital Micrograph 3.3. software.

2.3. Epoxidation of Cyclohexene. The catalysts were dried at 500 °C under dry air for 1 h prior to use. Typically, the catalyst (100 mg) was added to a solution of cyclohexene (1 mmol, Aldrich) in 5 mL of anhydrous acetonitrile (dried over 3A zeolites). The reaction mixture was heated and stirred at 85 °C in closed glass reactor and a solution of H_2O_2 (50% aqueous solution; Riedel-de-Haen; 0.2 mmol of H_2O_2 in 0.72 mL of solution) was dropwise added (0.01 mL min^{-1}) with an automatic dosimetric apparatus. Mesitylene was added as internal standard. Catalytic performance was determined via GC analysis (HP6890; HP-5 30 m column; FID detector). Yields were computed according to the relation

$$\text{Y epox} = [\text{mol(obtained epoxide)}/\text{mol(initial } H_2O_2)] \times 100$$

using pure standards to evaluate the GC response factors. Routinary heterogeneity tests were performed (hot filtration and separation of the solid catalysts) to ascertain the heterogeneous character of the catalysts and to exclude catalytic activity of homogeneous Ti species leached out from the catalyst.

2.4. Immersion Calorimetry. Immersion calorimetry measurements into cyclohexene (Fluka, 99%) taking part in the subsequent reaction processes were performed in a Setaram Tian-Calvet C80D calorimeter at 30 °C. Prior to the experiment, the samples were degassed in a glass-made vacuum equipment down to 10^{-3} Pa at 250 °C for 4 h. After degassing, the glass bulb containing the sample was sealed in vacuum and inserted into the calorimetric chamber containing the immersion liquid. Once thermal equilibrium is reached, the brittle tip of the glass bulb is broken and the heat of interaction is recorded as a function of time. The total enthalpy of immersion ($-\Delta H_{imm}$) is obtained by integration of the signal, after appropriate corrections of (i) the breaking of the tip (exothermic) and (ii) the heat of evaporation of the immersion liquid necessary to fill the empty volume of the bulb with the vapor at the corresponding vapor pressure (endothermic). Both corrections were previously calibrated using empty glass bulbs with different volumes. Three repetitions were performed for each calorimetric measurement, with a final experimental error below 3−4%. A detailed description of the experimental setup can be found elsewhere.[19]

3. RESULTS AND DISCUSSION

3.1. Characteristics of the Titanosilicate Catalysts. The most important structural characteristics of the different Ti-containing siliceous catalysts are summarized in Table 1. For comparison, the characteristics of the parent support materials MCM-41 and SBA-15 for Ti-MCM-41 and SBA-TS-15, respectively, are added. The characteristics of TS-1 and Ti-MCM-41 are comparable to the data reported in the literature.[1,30] The results of the porosimetric analysis of both SBA-TS-15 materials clearly show that the surface area, total pore volume, and micropore volume decreased significantly in comparison with the parent SBA-15 material, which is caused by the deposition of TS-1 nanoparticles in the inner mesoporous channels. Moreover, there are large structural differences between SBA-TS-15-pH 1 and SBA-TS-15-pH 13. The N_2-sorption isotherms (Figure 1) of both SBA-TS-15 materials have clearly changed as compared to the original SBA-15. In the case of SBA-TS-15-pH 13, there is a two-step desorption, which implies that there are two types of pores, namely narrowed and open pores. The isotherm is analogous to the one of "plugged hexagonal templated silica" (PHTS),[31] indicating that there are TS-1-like plugs deposited in the mesochannels of SBA-15. A schematic representation of the structure of SBA-TS-15-pH 13 is shown as an inset in Figure 1. Similar two-step desorption isotherms have been described in the literature for SBA-15 materials with pore constrictions after *n*-nonane preadsorption.[32] SBA-TS-15-pH 1, on the other hand, gives rise to a one-step desorption branch and an H_2 hysteresis, indicating the presence of ink-bottle pores. Moreover, the pore diameter of SBA-TS-15-pH 1 is decreased significantly in comparison with the parent SBA-15 material (Table 1), meaning that there is a coating inside the channels of SBA-15. A schematic representation of the SBA-TS-15-pH 1 structure can be found as an inset in Figure 1. In the case of SBA-TS-15-pH 13, the pore diameter also diminishes, but the decrease is less evident compared to SBA-TS-15-pH 1. This small reduction in pore diameter of SBA-TS-15-pH 13 can be due to the redeposition of dissolved amorphous silica of SBA-15, since its solubility is relatively high at pH 13.[33] At pH 1, on the other hand, dissolution of amorphous silica is unlikely,[33] and changes in the pore radius can be directly correlated to the deposited TS-1 nanoparticles. Thus, the pH of the TS-1 nanoparticles solution has a large influence on the structural characteristics of the resulting SBA-TS-15 material. It is noteworthy that both SBA-TS-15 materials do not show any zeolitic features (Table 1), which implies that the TS-1 nanoparticles solution is not able to induce XRD-detectable zeolitic features in the SBA-TS-15 materials.

Meso-TSM is a newly developed material, synthesized by applying a one-pot templating approach, whereby two types of structure directing agents, TPAOH and CTMABr, are added to the same reaction mixture in order to form simultaneously micro- and mesopores. According to N_2-sorption and XRD measurements

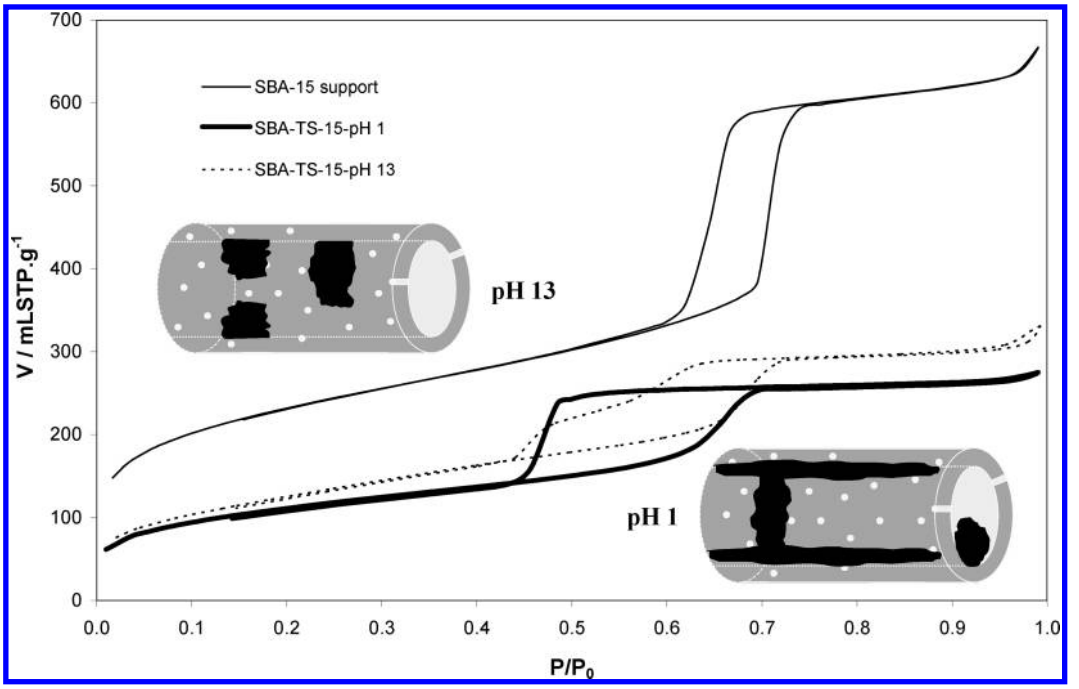

Figure 1. N_2-sorption isotherms ($T = -196$ °C) of SBA-15, SBA-TS-15-pH 1, and SBA-TS-15-pH 13. Schematic representations of the structure of SBA-TS-15-pH 1 and SBA-TS-15-pH 13 are added to the graph.

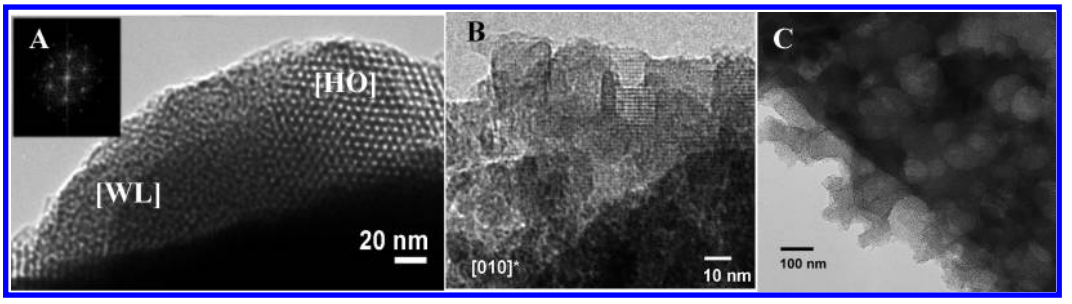

Figure 2. HR-TEM images of meso-TSM with (A) mesoporous region, partly hexagonally ordered [HO], partly wormlike [WL], (B) zeolitic particles at the edges of the mesoporous part, and (C) the macroholes.

(Table 1), meso-TSM has both mesoporous (type IV isotherm, analogues to MCM-41) and MFI zeolitic features (MFI zeolite profile). Moreover, the XRD pattern shows a narrow (100) band at 1.9° and a broad one [(110) and (200)] at 4.1° 2θ, which suggest a hexagonally ordered MCM-41 structure. However, a pure, well-ordered MCM-41 structure gives rise to four characteristic peaks in the 0° until 6° 2θ region,[34,35] so this indicates a locally disordered/nonpure MCM-41 structure. HR-TEM confirms these conclusions (Figure 2): the mesophase is partly hexagonally ordered and partly wormlike (Figure 2A). In addition, zeolitic particles can be detected at the edges of the mesoporous regions (Figure 2B). Thus, meso-TSM is a combined zeolitic/mesoporous composite material and not a true hierarchical mesoporous zeolite. Moreover, HR-TEM also reveals a special feature on the macroporous scale (Figure 2C). Throughout the entire meso-TSM structure, macroholes can be observed. These macroholes seem to be organized in a layered, sheetlike configuration: the darker and lighter contrast is originating from overlapping layers of macroholes which are shifted in-plane with respect to each other. The presence of the macroholes might be beneficial for catalytic applications, since reactants might diffuse more easily through these macroholes and reach the active sites more rapidly.

Another very important structural aspect of these materials is the concentration of active sites (Ti) in the structure of the catalysts. The Ti content of the different materials was determined by electron probe microanalysis (EPMA) (Table 1). The TS-1 microporous titanosilicate contains the highest amount of Ti, whereas the Ti content of SBA-TS-15-pH 1 is rather low. This can be due to the high solubility of TiO_x at low pH (leaching phenomenon).[36] EDX (not shown) points out that the Ti sites in meso-TSM (1.2%) are dispersed homogeneously throughout the entire structure, meaning that Ti is incorporated in the mesoporous as well as in the zeolitic parts of the meso-TSM structure.

Next to the concentration, the coordination of the active sites is also important, since tetrahedrally coordinated Ti is expected to be most efficient in the epoxidation reaction.[37−40] UV−vis (DR) spectra are shown in Figure 3. The position of the bands is related to the coordination of the Ti species.[37,41,42] The band centered at 210−220 nm is assigned to isolated tetrahedrally coordinated Ti species whereas a band between 250 and 290 nm is associated with penta- or hexacoordinated (oligomeric) Ti. Finally, crystalline TiO_2 anatase domains give rise to a band at 330 nm and upward. The latter has a negative effect on redox reactions using H_2O_2 as an oxidant because extraframework

dx.doi.org/10.1021/la104808v |*Langmuir* 2011, 27, 3618–3625

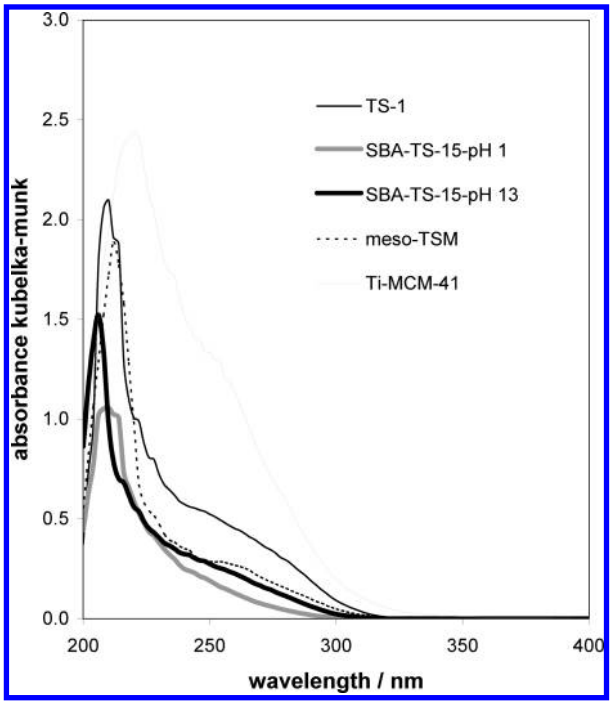

Figure 3. UV−vis (DR) spectra of the different titanosilicates.

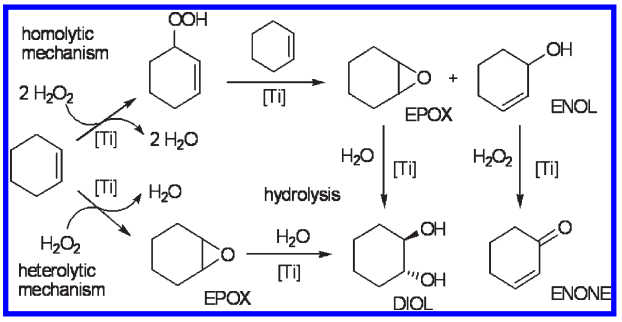

Figure 4. Schematic representation of the two different reaction pathways for the epoxidation of cyclohexene.

TiO_2 can cause the undesirable and useless decomposition of H_2O_2.[43] All titanosilicates give rise to a large, narrow band centered between 210 and 220 nm, which indicates that all materials have isolated tetrahedrally coordinated Ti in their structure. Second, the materials show a broad adsorption between 250 and 290 nm, which implies that there are also oligomeric penta- or hexacoordinated Ti−O−Ti species present. Especially Ti-MCM-41 contains a large fraction of oligomeric species in comparison with the other titanosilicates. Moreover, Ti-MCM-41 shows a very small absorption at $\lambda > 300$ nm, which suggests the presence of a very small amount of TiO_2-like clusters.

3.2. Epoxidation of Cyclohexene. Figure 4 depicts the two different reaction pathways for the epoxidation of cyclohexene with H_2O_2 as oxidant. The reaction can proceed via two routes: (1) a homolytic mechanism governed by free-radical species, leading mainly to the formation of allylic oxidation products (cyclohexanol and cyclohexanone); (2) a heterolytic oxygen transfer from H_2O_2, leading to the formation of epoxide (the desired product), that is promoted by the presence of well-isolated, accessible Ti active sites in the catalyst. Notice that the

Table 2. Catalytic Test Results for the Different Titanosilicate Catalysts in the Epoxidation of Cyclohexene[a]

	yield EPOX[b] (%)	sel EPOX[c] (%)	sel ENOL[c] (%)	sel ENONE[c] (%)
TS-1	1	31	49	20
Ti-MCM-41	51	91	5	4
SBA-TS-15-pH 1	4	49	42	9
SBA-TS-15-pH 13	3	50	42	8
meso-TSM	22	76	10	13

[a] EPOX = cyclohexene epoxide; ENOL = cyclohex-2-enol; ENONE = cyclohex-2-enone. [b] Yield of EPOX at the end of the dropwise (0.01 mL min^{-1}) H_2O_2 addition (after 1.2 h). [c] Selectivity toward EPOX, ENOL, or ENONE at the end of the dropwise (0.01 mL min^{-1}) H_2O_2 addition (after 1.2 h).

epoxide can easily react with H_2O, resulting in the formation of the diol as secondary product. The catalytic test results for the different titanosilicates are listed in Table 2. When taking into account the yield to epoxide, it is clear that the order of activity of the titanosilicates is Ti-MCM-41 ≫ meso-TSM ≫ SBA-TS-15-pH 1 ≥ SBA-TS-15-pH 13 > TS-1 ≈ 0. TS-1 shows very little activity in the epoxidation of cyclohexene, which is not surprising since cyclohexene is bulky and the oxygen transfer between the oxidant and the alkene cannot occur in the micropore network.[37,44−46] The epoxidation can only take place at the active sites on the external surface of the microporous titanosilicate due to diffusion limitations/restricted accessibility for cyclohexene. Ti-MCM-41, on the other hand, shows the best performance of all catalysts, and the obtained catalytic test results are similar to the data previously reported by Guidotti et al. under comparable conditions.[47] Here, cyclohexene molecules are able to reach and interact with all active sites of the catalyst; no diffusion limitations or restricted accessibility are being encountered. It is worth noting that the only material with a relative large amount of oligomeric Ti species, and even a small number of TiO_2-like clusters next to isolated tetrahedrally coordinated Ti (Figure 3), namely Ti-MCM-41, gives rise to the highest activity of all catalysts. Such behavior is a further suggestion that perfectly isolated and dispersed Ti(IV) centers are not necessarily the unique sites suitable for epoxidation of olefins.[48−50] The three types of combined zeolitic/mesoporous materials lie between the two extremes TS-1 and Ti-MCM-41. Both SBA-TS-15 materials show a similar activity, which tends toward the value of TS-1. These results suggest that cyclohexene is only reacting on the outer surface of the TS-1-like plugs or coating, in the case of SBA-TS-15-pH 13 and SBA-TS-15-pH 1, respectively. Moreover, it can also be concluded that the large structural differences between SBA-TS-15-pH 1 and SBA-TS-15-pH 13 do not have any notable influence on the catalytic tests, as the activity of both of them is poor. The activity of meso-TSM is much better than for the SBA-TS-15 materials. However, in comparison with the Ti-grafted MCM-41, meso-TSM displays a rather intermediate activity. This can be explained by the fact that meso-TSM is a combined zeolitic/mesoporous material with Ti dispersed homogenously throughout the entire structure. Since the catalytic data for TS-1 clearly show that this microporous material is not able to catalyze the epoxidation properly, it can be concluded that also in meso-TSM the Ti-containing zeolitic particles do not participate in the catalysis due to the restricted access of the cyclohexene molecule. Therefore, the only active sites that can interact with the cyclohexene molecules are the ones in the

dx.doi.org/10.1021/la104808v |*Langmuir* 2011, 27, 3618–3625

Table 3. Enthalpy of Immersion, with Cyclohexene as Immersion Liquid, for the Different Titanosilicates (J/g of Solid)

	$-\Delta H_{imm}$ (J g^{-1})		$-\Delta H_{imm}$ (J g^{-1})
TS-1	62	SBA-TS-15-pH 1	133
Ti-MCM-41	245	SBA-TS-15-pH 13	106
SBA-15 support	93	meso-TSM	159

mesoporous regions and at the outer surface/edges of the zeolitic domains. The presence of macroholes, even if it may play a positive role in improving the diffusion of the reactant molecules, does not seem to be crucial in this reaction under the conditions tested.

The selectivity values give a clear indication about the reaction pathway that is involved in the epoxidation. The order of selectivity for the epoxide is Ti-MCM-41 > meso-TSM > SBA-TS-pH 1 ≈ SBA-TS-15-pH 13 > TS-1. In the case of Ti-MCM-41, the selectivity for the epoxide is 91%, which means that the reaction occurs mainly via the heterolytic pathway. In the case of meso-TSM as catalyst, the production of the epoxide is preferential, even if the formation of free-radical products (enol−enone) is not negligible. Here, the reaction also predominantly proceeds via the heterolytic pathway. For TS-1 and the SBA-TS-15 materials, on the other hand, the selectivity to epoxide is much lower, and the large formation of enol−enone indicates that a large fraction of H_2O_2 reacted via the homolytic mechanism, most likely on defective sites on the outer surface. From the catalytic experiments, it is clear that the combined zeolitic/mesoporous materials described in this paper do not offer catalytic advantages compared to conventional Ti-grafted MCM-41 in terms of activity or selectivity. Concerning the subsequent reaction process, i.e., the opening of the epoxide ring by H_2O, Ti-MCM-41 and meso-TSM materials show a scarce formation of 1,2-cyclohexanediol in the reaction mixture, as observed by GC analysis. However, at the end of the reaction time, remarkable amounts of diol are detected on the surface of the solids by TGA and solid-state ^{13}C-MAS NMR (as already evidenced in a previous work[47]), indicating a strong interaction of highly polar (dihydroxy) species with the surface of the catalysts.

3.3. Immersion Calorimetry. According to the literature, not only the number of active sites but also the surface chemistry of the titanosilicates is an important factor defining the degree of interaction of the different reactants and products with the solid surface and, consequently, its behavior in terms of activity and selectivity in the epoxidation of olefins.[51−53] Furthermore, in the absence of moisture the direct interaction of the olefin with the active sites on the surface is the rate-determining step with the reaction rate to the epoxide scaling with the concentration of olefins in the reaction mixture.[54,55] Since the titanosilicate materials all have similar active sites involved in catalysis (mainly exposed isolated titanium sites in predominantly tetrahedral coordination; see section 3.1), the interaction of the olefin with the catalytic surface seems to play a defining role in the final catalytic activity. This implies that learning more about this interaction could lead to important insight into the catalytic activity of the materials. A suitable technique to quantify the interaction between a solid surface and a liquid molecule is immersion calorimetry.

The values for the enthalpy of immersion (J/g^{-1}) in pure cyclohexene for the different titanosilicate catalysts are shown in Table 3. The enthalpy or heat of immersion reflects the degree of interaction between the immersion liquid and the catalyst. Since in this study the immersion liquid is also the reactant in the epoxidation reaction, $-\Delta H_{imm}$ represents the degree of interaction between the reactant and the solid surface, which indirectly measures the nature of the active sites. This means that the higher the enthalpy value, the larger the interaction of cyclohexene with the catalyst's surface. The order of interaction is Ti-MCM-41 > meso-TSM > SBA-TS-15-pH 1 > SBA-TS-15-pH 13 > TS-1. This order completely correlates to the order of the catalytic activity in the epoxidation reaction, catalyzed by the different titanosilicates. The lowest enthalpy corresponds to TS-1, which is not surprising since cyclohexene is not able to enter the pores of this microporous titanosilicate. This results in quite a low degree of interaction, leading toward a low catalytic activity. Ti-MCM-41 gives rise to a very high heat of immersion, thus reflecting the absence of accessibility problems and the high degree of interaction between its surface and the cyclohexene molecules. Moreover, Ti-MCM-41 is the only catalyst that experienced a color change during the immersion experiment. The white catalyst became yellow, which could indicate a specific interaction between cyclohexene and Ti. Indeed, Ti has d-orbitals which can coordinate with the π electrons of the cyclohexene molecule, through the double bond, thus producing a coordination compound.[37] However, the presence of associated isomerization reactions as a result of this interaction cannot be ruled out to account for the large heat of immersion. In the case of the combined zeolitic/mesoporous materials, the order of the enthalpy values also coincides with the order of catalytic activity. In the case of the SBA-TS-15 materials (and besides the decrease in the specific surface area compared to the parent SBA-15 structure), the enthalpy value increases significantly after the deposition of TS-1 nanoparticles on the SBA-15 support, indicating that the TS-like plugs/coating exhibit a large influence on the interaction with cyclohexene. However, although the immersion calorimetry experiments and the epoxidation reaction follow the same trend, the difference in enthalpy values for the two types of SBA-TS-15 materials is larger than their difference in catalytic activity, which is almost negligible. This discrepancy must be attributed to the low conversion levels of cyclohexene achieved under reaction conditions on these combined zeolitic/mesoporous materials, whereby the experimental error gives rise to a large uncertainty in the comparison among different samples.

In summary, immersion calorimetry measurements on different titanosilicates and using cyclohexene as probe molecule show that the enthalpy of immersion nicely correlates with the catalytic activity of these materials in the epoxidation of the aforementioned molecule. Incorporation of Ti in the structure of these materials gives rise to an improvement in the degree of interaction and in the catalytic activity when compared to the pure siliceous counterpart. Consequently, immersion calorimetry is a good technique to quantify the interaction between the reactant, i.e., cyclohexene, and the catalyst surface. Moreover, since the interaction of cyclohexene with the titanosilicate catalysts is a crucial step in the epoxidation reaction, immersion calorimetry in cyclohexene can be proposed as an easy/simple technique for the characterization and fast evaluation of different micro- and/or mesoporous catalysts in the aforementioned reaction. However, generalizing the use of immersion calorimetry as an easy screening tool for catalysts needs to be done with care. Immersion calorimetry in a pure liquid does not take into account concurrent factors taking place during a catalytic reaction, such as the competitive adsorption of other reactants or reaction products, or the poisoning (or fouling) of the catalyst. In fact, only in those

reactions where the interaction/adsorption of the reactant (probe molecule) with the solid catalyst is a determining factor for the catalytic activity of the material (= rate-determining step in the catalysis), immersion calorimetry into this probe molecule has great potential as a fast evaluation technique.

4. CONCLUSIONS

Different types of titanosilicate materials have been fully structurally characterized and subsequently evaluated for the epoxidation of cyclohexene. Next to the more conventional materials, TS-1 and Ti-MCM-41, three types of combined zeolitic/mesoporous materials (meso-TSM, SBA-TS-15-pH 1, SBA-TS-15-pH 13) have been applied as catalyst. The order of catalytic activity is Ti-MCM-41 ≫ meso-TSM ≫ SBA-TS-15-pH 1 ≥ SBA-TS-15-pH 13 > TS-1. The catalytic test results have been correlated with the different structural properties of the titanosilicates and with the immersion calorimetry results using cyclohexene as immersion liquid. Immersion calorimetry was performed in order to evaluate the interaction between the reactant (cyclohexene) and the catalyst (titanosilicate), which is a crucial factor in the epoxidation reaction. It turned out that the trend in immersion enthalpy completely correlated with the order of catalytic activity for the different catalysts. This paper has therefore demonstrated for the very first time that the combination of catalytic testing and immersion calorimetry, when using the same molecule, can lead to important insights into the influence of the different materials characteristics on the catalytic behavior. Immersion calorimetry can hence be used as an auxiliary characterization tool for a better understanding of the interaction between the solid catalyst and the substrate. More specifically, immersion calorimetry with cyclohexene can be applied as a screening tool for the catalytic epoxidation of cyclohexene. Nevertheless, it should be kept in mind that immersion calorimetry can only serve as an adequate screening tool (with a straightforward interpretation) for catalysts, when the adsorption of the molecules used as immersion liquid is the rate-determining step in the catalytic reaction.

AUTHOR INFORMATION

Corresponding Author

*E-mail jarian.vernimmen@ua.ac.be, tel +32 3 265 23 79, fax +32 3 265 23 74.

ACKNOWLEDGMENT

J. Vernimmen thanks the Fund for Scientific Research-Flanders (FWO-Vlaanderen) for financial support. The Concerted Research Project (CRP, GOA-project) sponsored by the Special Fund for Research at the University of Antwerp is acknowledged. The networks of Excellence (EU-FP6), INSIDE-PORES and IDECAT, are gratefully acknowledged. R. Psaro and M. Guidotti acknowledge financial support from the European Community's 7th Framework Programme through the Marie Curie Initial Training Network NANO-HOST (Grant Agreement no. 215193) and from the Italian Ministry of Education, University and Research through the Project "ItalNanoNet" (prot. no. RBPR05JH2P).

REFERENCES

(1) Taramasso, M.; Perego, G.; Notari, B. US Patent 4,410,501, 1983.
(2) Cavani, F.; Teles, J. H. *ChemSusChem* **2009**, *2*, 508–534.
(3) Guisnet, M.; Guidotti, M. *Zeolite Chemistry and Catalysis. An Integrated Approach and Tutorial*; Springer: Berlin, 2009; pp 275−347.
(4) Romano, U.; Esposito, A.; Maspero, F.; Neri, C.; Clerici, M. G. *Stud. Surf. Sci. Catal.* **1990**, *55*, 33–41.
(5) Liu, H.; Lu, G.; Guo, Y.; Guo, Y. *Appl. Catal., A* **2005**, *293*, 153–161.
(6) Thangaraj, A.; Kumar, R.; Ratnasamy, P. *J. Catal.* **1991**, *131*, 294–297.
(7) Kumar, R.; Mukherjee, P.; Bhaumik, A. *Catal. Today* **1999**, *49*, 185–191.
(8) Bhaumik, A.; Tatsumi, T. *Chem. Commun.* **1998**, 463–464.
(9) Maspero, F.; Romano, U. *J. Catal.* **1994**, *146*, 474–482.
(10) Cundy, C. S.; Forrest, J. O. *Microporous Mesoporous Mater.* **2004**, *72*, 67–80.
(11) Tvaruzkova, Z.; Zilkova, N. *Appl. Catal., A* **1993**, *103*, L1–L4.
(12) Clerici, M. G. *Metal Oxide Catalysis*; Wiley-VCH: Berlin, 2009; pp 705−754.
(13) Taguchi, A.; Schüth, F. *Microporous Mesoporous Mater.* **2005**, *77*, 1–45.
(14) Corma, A. *Chem. Rev.* **1997**, *97*, 2373–2419.
(15) Cassiers, K.; Linssen, T.; Mathieu, M.; Benjelloun, M.; Schrijnemakers, K.; Van Der Voort, P.; Cool, P.; Vansant, E. F. *Chem. Mater.* **2002**, *14*, 2317–2324.
(16) Poladi, R. H. P. R.; Landry, C. C. *Microporous Mesoporous Mater.* **2002**, *52*, 11–18.
(17) Meng, X.; Li, D.; Yang, X.; Yu, Y.; Wu, S.; Han, Y.; Yang, Q.; Jinag, D.; Xiao, F.-S. *J. Phys. Chem. B* **2003**, *107*, 8972–8980.
(18) Lin, K.; Sun, Z.; Lin, S.; Jiang, D.; Xiao, F.-S. *Microporous Mesoporous Mater.* **2004**, *72*, 193–201.
(19) Silvestre-Albero, J.; Gómez de Salazar, C.; Sepúlveda-Escribano, A.; Rodriguez-Reinoso, F. *Colloids Surf., A* **2001**, *187−188*, 151–165.
(20) Denoyel, R. *Colloids Surf., A* **2002**, *205*, 61–71.
(21) López-Ramón, M. V.; Stoeckli, F.; Moreno-Castilla, C.; Carrasco-Marín, F. *Carbon* **2000**, *38*, 825–829.
(22) Guerfi, K.; Lagerge, S.; Meziani, M. J.; Nedellec, Y.; Chauveteau, G. *Thermochim. Acta* **2005**, *434*, 140–149.
(23) Meziani, M. J.; Zajac, J.; Douillard, J.-M.; Jones, D. J.; Partyka, S.; Roziére, J. *J. Colloid Interface Sci.* **2001**, *233*, 219–226.
(24) Silvestre-Albero, A.; Ramos-Fernández, J. M.; Martínez-Escandell, M.; Sepúlveda-Escribano, A.; Silvestre-Albero, J.; Rodriguez-Reinoso, F. *Carbon* **2010**, *48*, 548–556.
(25) Molina-Sabio, M.; Rodríguez-Reinoso, F.; González, M. T. *Langmuir* **1997**, *13*, 2354–2358.
(26) Costarrosa, L.; Ruiz-Martínez, J.; Rios, R.V.R.A.; Silvestre-Albero, J.; Rojas-Cervantes, M. L.; Sepúlveda-Escribano, A. *Microporous Mesoporous Mater.* **2009**, *120*, 115–121.
(27) Meynen, V.; Cool, P.; Vansant, E. F.; Kortunov, P.; Grinberg, F.; Kärger, J.; Mertens, M.; Lebedev, O. I.; Van Tendeloo, G. *Microporous Mesoporous Mater.* **2007**, *99*, 14–22.
(28) Liu, S.; Cool, P.; Collart, O.; Van Der Voort, P.; Vansant, E. F.; Lebedev, O. I.; Van Tendeloo, G.; Jiang, M. *J. Phys. Chem. B* **2003**, *107*, 10405–10411.
(29) Guidotti, M.; Ravasio, N.; Psaro, R.; Ferraris, G.; Moretti, G. *J. Catal.* **2003**, *214*, 242–250.
(30) Guidotti, M.; Batonneau-Gener, I.; Gianotti, E.; Marchese, L.; Mignard, S.; Psaro, R.; Sgobba, M.; Ravasio, N. *Microporous Mesoporous Mater.* **2008**, *111*, 39–47.
(31) Van Der Voort, P.; Ravikovitch, P. I.; De Jong, K. P.; Benjelloun, M.; Van Bavel, E.; Janssen, A. H.; Neimark, A. V.; Weckhuysen, B. M.; Vansant, E. F. *J. Phys. Chem. B* **2002**, *106*, 5873–5877.
(32) Silvestre-Albero, A.; Jardim, E. O.; Bruijn, E.; Meynen, V.; Cool, P.; Sepúlveda-Escribano, A.; Silvestre-Albero, J.; Rodríguez-Reinoso, F. *Langmuir* **2009**, *25*, 939–943.
(33) Iler, R. K. *The Chemistry of Silica: Solubility, Polymerization, Colloid and Surface Properties, and Biochemistry*; John Wiley & Sons: New York, 1976; p 42.
(34) Beck, J. S.; Vartuli, J. C.; Roth, W. J.; Leonowicz, M. E.; Kresge, C. T.; Schmitt, K. D.; Chu, C. T.-W.; Olson, D. H.; Sheppard, E. W.;

McCullen, S. B.; Higgins, J. B.; Schlenker, J. L. *J. Am. Chem. Soc.* **1992**, *114*, 10834–10843.
(35) Meynen, V.; Cool, P.; Vansant, E. F. *Microporous Mesoporous Mater.* **2009**, *125*, 170–223.
(36) Baes, C. F., Jr.; Mesmer, R. E. *The Hydrolysis of Cations*; John Wiley & Sons: New York, 1976; p 150.
(37) Ratnasamy, P.; Srinivas, D.; Knozinger, H. *Adv. Catal.* **2004**, *48*, 1–169.
(38) Marchese, L.; Gianotti, E.; Dellarocca, V.; Maschmeyer, T.; Rey, F.; Coluccia, S.; Thomas, J. M. *Phys. Chem. Chem. Phys.* **1999**, *1*, 585–592.
(39) Bordiga, S.; Damin, A.; Bonino, F.; Ricchiardi, G.; Lamberti, C.; Zecchina, A. *Angew. Chem., Int. Ed.* **2002**, *41*, 4734–4737.
(40) Barker, C. M.; Gleeson, D.; Kaltsoyoannis, N.; Catlow, C. R. A.; Sankar, G.; Thomas, J. M. *Phys. Chem. Chem. Phys.* **2002**, *4*, 1228–1240.
(41) Guidotti, M.; Ravasio, N.; Psaro, R.; Gianotti, E.; Coluccia, S.; Marchese, L. *J. Mol. Catal. A: Chem.* **2006**, *250*, 218–225.
(42) Gianotti, E.; Bisio, C.; Marchese, L.; Guidotti, M.; Ravasio, N.; Psaro, R.; Coluccia, S. *J. Phys. Chem. C* **2007**, *111*, 5083–5089.
(43) Notari, B. *Catal. Today* **2003**, *18*, 163–172.
(44) Corma, A.; Camblor, M. A.; Esteve, P.; Martinez, A.; Pérez-Pariente, J. *J. Catal.* **1994**, *145*, 151–158.
(45) Schmidt, I.; Krogh, A.; Wienberg, K.; Carlsson, A.; Brorson, M.; Jacobsen, C. J. H. *Chem. Commun.* **2000**, 2157–2158.
(46) Fan, W.; Wu, P.; Tatsumi, T. *J. Catal.* **2008**, *256*, 62–73.
(47) Guidotti, M.; Pirovano, C.; Ravasio, N.; Lázaro, B.; Fraile, J. M.; Mayoral, J. A.; Coq, B.; Galarneau, A. *Green Chem.* **2009**, *11*, 1421–1427.
(48) Bouh, A. O.; Rice, G. L.; Scott, S. L. *J. Am. Chem. Soc.* **1999**, *121*, 7201–7210.
(49) Kholdeeva, O. A.; Ivanchikova, I. D.; Guidotti, M.; Pirovano, C.; Ravasio, N.; Barmatova, M. V.; Chesalov, Y. A. *Adv. Synth. Catal.* **2009**, *351*, 1877–1889.
(50) Lundin, A.; Panas, I.; Ahlberg, E. *J. Phys. Chem. A* **2009**, *113*, 282–290.
(51) Corma, A.; Domine, M.; Gaona, J. A.; Jorda, J. L.; Navarro, M. T.; Rey, F.; Pérez-Pariente, J.; Tsuji, J.; McCulloch, B.; Nemeth, L. T. *Chem. Commun.* **1998**, 2211–2212.
(52) Blasco, T.; Corma, A.; Navarro, M. T.; Pérez Pariente, J. *J. Catal.* **1995**, *156*, 65–74.
(53) Blasco, T.; Camblor, M. A.; Corma, A.; Esteve, P.; Guil, J. M.; Martínez, A.; Perdigón-Melón, J. A.; Valencia, S. *J. Phys. Chem. B* **1998**, *102*, 75–88.
(54) Domine, M. E. Sólidos ácidos de Lewis como catalizadores heterogéneos en reacciones de oxidación de interés en química fina. PhD Thesis, UPV, Valencia, Spain.
(55) Bouh, A. O.; Hassan, A.; Scott, S. L. *Catalysis of Organic Reactions*; Marcel Dekker: New York, 2003; pp 537−543.